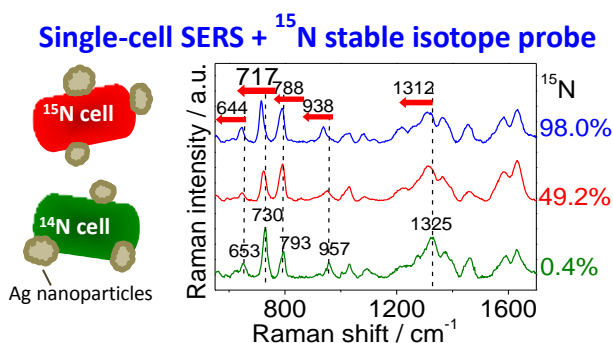


Surface-enhanced Raman spectroscopy combined with stable isotope probing to monitor nitrogen assimilation at both bulk and single-cell level

Li Cui,^{*,†,‡} Kai Yang,[†] Guowei Zhou,[†] Wei E. Huang,^{*,‡} Yong-Guan Zhu[†]

[†]Key Lab of Urban Environment and Health, Institute of Urban Environment, Chinese Academy of Sciences, Xiamen 361021, China. [‡]Department of Engineering Science, University of Oxford, Oxford, OX1 3PJ, UK.

TOC/Abstract art



1 **ABSTRACT**

2 Microbe-mediated biogeochemical cycle of nitrogen is a critical process in the
3 environment. In this study, surface-enhanced Raman spectroscopy combined with ^{15}N
4 stable isotope probing (SERS- ^{15}N SIP) was developed as a new, non-destructive, and
5 robust approach to probe nitrogen assimilation by bacteria at both bulk and single-cell
6 level, and from pure culture to environmental microbial community. Multiple
7 distinguishable SERS band shifts were observed and displayed a linear relationship with
8 ^{15}N content, due to the substitution of 'light' nitrogen by 'heavier' ^{15}N stable isotope.
9 These shifts, especially in 730 cm^{-1} band, were highly distinguishable and universal in
10 different bacteria, providing a robust indicator for nitrogen assimilation in bacteria.
11 SERS- ^{15}N SIP was also demonstrated in important N_2 -fixing bacteria via $^{15}\text{N}_2$ incubations.
12 The same prominent shifts as that induced by $^{15}\text{NH}_4\text{Cl}$ were observed, indicating the
13 applicability of SERS- ^{15}N SIP to different nitrogen sources. SERS- ^{15}N SIP was further
14 applied to environmental microbial community via $^{15}\text{NH}_4\text{Cl}$, $^{15}\text{NO}_3$, and $^{15}\text{N}_2$ incubation.
15 Bacteria- and nitrogen source-dependent activity in nitrogen assimilation were revealed
16 in environmental microbial community, pointing to the bacterial diversity and necessity
17 of single-cell level investigation. Finally, by mixing optimized ratio of bacteria with Ag
18 NPs, explicit single-cell SERS- ^{15}N SIP was obtained. The non-destructive SERS- ^{15}N SIP
19 approach will be useful not only to identify active nitrogen-assimilating cells, but also
20 enable Raman activated cell sorting and down-stream genomic analysis, which will bring
21 in deep insights into nitrogen metabolism of environmental microorganisms.

22 **KEYWORDS:** nitrogen assimilation, N_2 -fixation, ^{15}N stable isotope probing (SIP),
23 surface-enhanced Raman spectroscopy, single cell

1 INTRODUCTION

2 Nitrogen (N) is an essential element sustaining life on the earth. Microorganisms
3 (bacteria and archaea)-mediated biogeochemical nitrogen cycle is a critical process to
4 convert nitrogen to various bioavailable chemical forms.¹⁻³ Due to the lack of radioactive
5 nitrogen, stable isotope labelling of ^{15}N is one of the most important methods to
6 investigate microbe-related nitrogen processes. For instance, incubation with $^{15}\text{N}_2$ has
7 been used to identify active N_2 -fixation microbes in soil and compare their activity based
8 on ^{15}N enrichment.^{2,3} Assimilation of $^{15}\text{NH}_4^+$ was used to investigate the anabolic activity
9 of archaea and bacteria.⁴ Extremely slow-growing anaerobic methanotrophs can be
10 monitored by ^{15}N assimilation.⁵

11 Mass spectrometer is predominantly employed to detect ^{15}N -labeled cells or their
12 metabolites due to its high sensitivity to quantify very low stable isotope incorporation.²⁻⁶
13 However, because vast majority of microorganisms are nonculturable and highly
14 heterogeneous within a microbial community,⁷ and measurement of bulk microbial
15 activities is hard to define functionality and ecological roles of some key bacteria in
16 microbiota.⁸ Secondary ion mass spectrometry (NanoSIMS) can achieve single-cell
17 resolution and thus has been applied to reveal anabolic activity of single bacteria and
18 archaea within a nonculturable methane-oxidizing syntrophic consortia by measuring ^{15}N
19 assimilation,⁴ and to identify microorganisms contributing to N_2 -fixation in soil and
20 intertidal microbial mats.^{2,3} However, mass spectroscopy including NanoSIMS is a
21 destructive technique, preventing cells of interest from down-stream studies such as
22 single-cell genomics and even cultivation.

23 Raman spectroscopy has been demonstrated to be an attractive alternative for

1 non-destructive analysis of isotope-labelled microorganisms at single-cell level.⁹⁻¹¹
2 Raman spectra can provide intrinsic, label-free and rich information of various
3 biomolecules in cells, including proteins, nucleic acids, lipids and carbohydrate.^{12,13} More
4 importantly, cells assimilating isotopic atoms display significant shifts in Raman bands
5 due to the substitution of 'light' atom in a chemical bond by its 'heavier' isotope. The
6 shift can not only be used to probe substrate (e.g., ¹³C-carbon) metabolism in single cell,
7 but also to reveal ecological function (e.g., indication of metabolic activity by
8 incorporation of ²D) of single cell in their natural habitat.⁹⁻¹¹ The combination of
9 ¹³C-stable isotope labelled naphthalene with Raman spectroscopy has previously
10 identified nonculturable naphthalene-degrading bacteria from groundwater microbial
11 community.¹⁰ Sugar-specific activity of microbial cells in a mouse cecal microbiota were
12 also compared by tracking heavy water assimilation in cells using single-cell Raman
13 spectroscopy.⁹ Moreover, the non-destructive Raman detection also enabled recovering of
14 cells for subsequent single-cell genomics.^{9,14} Despite the importance of nitrogen
15 metabolism, ¹⁵N-induced Raman shifts were not so distinguishable as those induced by
16 ¹³C or ²D,^{9-11,15} and the reported differentiation of normal Raman spectra of ¹⁵N-labeled
17 bacteria had to rely on multivariate analysis such as principal component-discriminant
18 function analysis.¹⁵ This limits its application, especially for microbial community
19 containing diverse cells.

20 Surface-enhanced Raman spectroscopy (SERS) is able to provide very strong Raman
21 signals due to the electromagnetic enhancement from silver or gold nanoparticles (Ag or
22 Au NPs).^{16,17} SERS enhancement is selective and only those molecules strongly adsorbed
23 onto the surface of Ag or Au NPs can get greatly enhanced, resulting in different SERS

spectra from normal Raman spectra.^{10,15,18-25} Recently, aiming to elucidate the SERS band origin of bacteria, Premasiri et al. and Kubryk et al. acquired SERS spectra from bacteria cultured in $^{15}\text{NH}_4\text{Cl}$ and $^{14}\text{NH}_4\text{Cl}$ media, and observed obviously ^{15}N -induced shift in SERS bands without use of multivariate analysis,^{26,27} indicating the superiority of SERS over normal Raman in this regard. However, to develop SERS combined with ^{15}N stable isotope probing (SERS- ^{15}N SIP) as a new method to study nitrogen assimilation, reproducibility and robustness of the method have to be examined. More importantly, the applicability of SERS- ^{15}N SIP in different nitrogen sources such as N_2 assimilated specifically by important N_2 -fixing bacteria, and also application in environmental microbial community containing diverse bacterial species needs to be investigated.

In this work, SERS- ^{15}N SIP was investigated across four different types of bacteria under various enhancement conditions in order to examine the robustness, reproducibility and universality of SERS band shift in probing nitrogen assimilation. In addition, we also demonstrated the applicability of SERS- ^{15}N SIP in N_2 -fixation via ^{15}N incubation, and monitoring the activity of environmental microbial community from wetland water in assimilating different nitrogen sources including $^{15}\text{NH}_4\text{Cl}$, $^{15}\text{NO}_3$, and $^{15}\text{N}_2$. Finally, by optimizing the ratio of bacteria and Ag NPs, a high resolution single-cell SERS- ^{15}N SIP was achieved. These works will demonstrate that SERS- ^{15}N SIP can be used as a good means to study activity of highly diverse environmental microorganisms in nitrogen cycle.

MATERIALS AND METHODS

Media, bacterial species, and growth conditions. Minimal media (100 mL) were prepared by using 0.1 g of $^{14}\text{N-NH}_4\text{Cl}$ or $^{15}\text{N-NH}_4\text{Cl}$ (98 atom % ^{15}N , Sigma-Aldrich, UK)

as nitrogen source, and other components including 0.25 g Na₂HPO₄, 0.25 g KH₂PO₄, 0.01 g MgSO₄·7H₂O, 1 µL of saturated CaCl₂ and FeSO₄ solution, and 0.1 mL Bauchop Elsdon solution.²⁸ ¹⁵N- and ¹⁴N-NH₄Cl-containing media were mixed at different ratios of 100:0, 75:25, 50:50, 25:75, 10:90, 5:95, 0:100. Considering that ¹⁵N content is 98% in commercial ¹⁵N-NH₄Cl and 0.4% in its natural abundance, the final ¹⁵N content in the growth media was 98.0%, 73.6%, 49.2%, 24.8%, 10.1%, 0.4%, respectively. To obtain various levels of ¹⁵NH₄Cl-labelled cells, *Escherichia coli* DH5α were grown in the above media with 10 mM glucose as the sole carbon source at 37 °C, *Pseudomonas putida* KT2440 were grown at 28 °C using sodium citrate as the sole carbon source, and gram-positive *Bacillus megaterium* KU647234 were grown at 37 °C using a mixture of 10 mM glucose, sodium succinate, and sodium citrate as the carbon source. To obtain deuterium-labelled or ¹³C-labelled *E.coli*, DH5α strain were grown in LB medium with 50% (vol/vol) D₂O (70 atom % D, Sigma-Aldrich), or in minimal media with ¹³C-glucose (99 atom % ¹³C, Sigma-Aldrich) as the carbon source.

Azotobacter chroococcum (ACCC10096) was used as a N₂-fixing bacterium. To culture it, 20 mL of azotobacter medium containing 0.2 g/L KH₂PO₄, 0.8 g/L K₂HPO₄, 0.2 g/L MgSO₄ 7H₂O, 0.1 g/L CaSO₄ H₂O, 20 g/L mannitol, and trace amount of Na₂MoO₄ 2H₂O and FeCl₃ were put in a 60-mL vial, purged with O₂ to remove air and then sealed. The headspace was then replaced with 32 mL ¹⁵N₂ (98.5% atom, Aladdin), producing a mixture gas comprising 80% N₂ and 20% O₂. Control culture contained lab air. *A. chroococcum* were cultured at 30°C.

Environmental microcosms were sampled from surface water of Xinglin Bay, which is the most important wetland in Jimei district of Xiamen city. After filtering using 10 and 3

1 μm microfiltration membrane to remove big particles, Xinglin Bay water was amended
2 with 10 mM glucose, sodium succinate, and sodium citrate as carbon source, and
3 $^{15}\text{NH}_4\text{Cl}$, $^{15}\text{NO}_3$, $^{15}\text{N}_2$ respectively as the nitrogen source, and then incubated at room
4 temperature.

5 All bacterial strains were harvested after overnight culture for Raman measurements.
6 Chemicals without explicitly stated were purchased from Sinopharm Chemical Reagent
7 Co., China.

8 **Nanoparticles preparation.** Ag (average size of 80 nm) and Au nanoparticles (average
9 size of 140 nm) were synthesized by reducing AgNO_3 and HAuCl_4 by trisodium citrate
10 respectively.²⁰ Detailed preparation procedure and characterization of nanoparticles can
11 be found in our previous works.^{20,29,30} The as-prepared Ag and Au NPs were washed once
12 by ultrapure water and concentrated through centrifugation at 6000 rpm and 2900 rpm for
13 5 min respectively. After the supernatant was discarded, the precipitate was collected, and
14 high concentration of Ag and Au NPs ranged between 4000 and 10000 mg/L were
15 obtained. All of the concentrated NPs were freshly prepared before each measurement.

16 **Bulk and single-cell SERS sample preparation.** To prepare bulk bacterial SERS
17 samples, overnight-cultured *E. coli*, *P. putida*, *B. megaterium*, *A. chroococcum* and
18 Xinglin Bay microorganisms were washed twice using ultrapure water by centrifugation
19 at 5000 rpm for 3 min. After removing supernatant, the cell pellets were mixed with 10
20 μL of concentrated Ag (~ 4200 mg/L) and/or Au (~ 9000 mg/L) thoroughly, and then 1 μL
21 of mixture was dropped onto a glass slide and air dried prior to SERS measurement. To
22 study effect of Ag NPs on bulk SERS spectra of bacteria, 200 μL of overnight-cultured
23 *E. coli* fed with 98.0%, 73.6%, and 0.4% $^{15}\text{N-NH}_4\text{Cl}$ were washed twice by ultrapure

1 water, and then mixed with different volumes of Ag NPs to reach a final concentration of
2 5, 10, 50, 70 mg/L respectively. 1 μ L of the mixture was dropped on a glass slide and air
3 dried. To prepare single-cell SERS sample, 10 μ L of two-fold diluted
4 overnight-cultured *E.coli* was washed twice by ultrapure water and then mixed with 10
5 μ L of concentrated Ag NPs (~7000 mg/L). An aliquot of 2 μ L of mixture was dropped on
6 a aluminum-coated glass slide and air dried.

7 **SERS measurement.** Bulk bacterial SERS spectra were acquired using a LabRAM
8 Aramis (HORIBA Jobin-Yvon) confocal micro-Raman system equipped with a 600 g/mm
9 grating. A 50 \times objective (Olympus) with a numerical aperture of 0.55 and a working
10 distance of 8 mm was used to focus the laser beam and collect Raman signal. Excitation
11 was provided by a He–Ne 632.8 nm laser with 0.7 mW power for all pure cultured
12 bacteria, and by a 532 nm Nd:YAG laser at laser power of 1 mW for Xinglin Bay
13 microorganisms due to the strong fluorescent background excited by 633 nm laser from
14 environmental sample. To minimize the possible damage to sample by the laser, Duoscan
15 in the micromapping mode with a scanning area of $30 \times 30 \mu\text{m}^2$ was used, based on the
16 combination of two mirrors scanning the laser beam rapidly across the chosen area.
17 Acquisition time of 4 s was applied. About eight SERS spectra from different areas of
18 one sample were acquired.

19 Single-cell SERS spectra were acquired using a LabRAM HR Evolution (HORIBA,
20 London, UK) confocal micro-Raman system equipped with a 532 nm Nd:YAG laser
21 (Ventus, Laser Quantum, Manchester, UK) at laser power of 20 μ W and a 600 g/mm
22 grating. The acquisition time was 3 s per cell. Single-cell normal Raman measurement
23 was performed using a 532 nm laser at laser power of 2 mW and 300 g/mm grating. A

1 100× magnifying dry objective ((NA = 0.90, Olympus, UK) was used to observe and
2 collect Raman signal from single cell.

3 **Spectral analysis.** LabSpec5 software (HORIBA Jobin-Yvon) was used to perform
4 baseline correction and peak fitting based on Gaussian (Lorentzian) formulas in order to
5 identify peak positions. The obtained peak positions were plotted against ^{15}N percentage
6 and linear fitting was then performed using Origin 8.5.1.

7 **RESULTS AND DISCUSSION**

8 **Establishment of SERS- ^{15}N SIP methodology to probe ^{15}N assimilation by bacteria**

9 Normal Raman spectra of ^2D , ^{13}C , ^{15}N isotope-labelled *E. coli* were displayed with the
10 unlabeled ones to compare the shifting extent induced by different stable isotopes (Figure
11 1). Raman spectra of ^2D - and ^{13}C -glucose labelled cells displayed a prominent shift from
12 2930 to 2160 cm^{-1} and 1002 to 967 cm^{-1} respectively. By comparison, shifts induced by
13 ^{15}N substitution were much less distinguishable in normal Raman spectra, because they
14 occurred in either weak bands (776, 720 cm^{-1}) that were masked in spectral noise or
15 unspecifically overlapping with other bands (1236, 1570 cm^{-1}).³¹ It is thus difficult to
16 explicitly identify ^{15}N -labelled cells using normal Raman spectra.

17 SERS spectra of bacteria displayed a very different feature with strong bands at 730,
18 793, 1325, 1581, 1632 cm^{-1} (Figure 2A), compared to the dominant bands at 1000, 1232,
19 1317, 1571, 1662 cm^{-1} in normal Raman spectra (Figure 1). This is due to the selective
20 enhancement effect of SERS to some biomolecules with strong binding affinity to Ag or
21 Au NPs.^{17,32} Interestingly, we found that Ag NPs-enhanced SERS spectra of ^{15}N -labeled
22 cells displayed clear characteristic shifts with increasing percentages of ^{15}N -ammonium
23 in medium (Figure 2). Among six shifted SERS bands from cells growing in minimal

1 medium with 98.0% ^{15}N - NH_4Cl , 730, 957, 1094, 1323 cm^{-1} bands displayed significant
2 shifts of 13, 19, 14 and 13 cm^{-1} , respectively; and 653 and 795 cm^{-1} bands displayed a
3 relatively small shift of 8.9 and 5.4 cm^{-1} respectively (Figure 2A).

4 To demonstrate the robustness and reproducibility of SERS method, SERS spectra of
5 ^{15}N -labeled *E. coli* were also obtained using Au NPs to enhance Raman signal (Figure
6 2B). Clear shifts were also observed at bands of 736 (13 cm^{-1} shift), 802 (6 cm^{-1} shift),
7 965 (~19 cm^{-1} shift), and 1325 cm^{-1} (13 cm^{-1} shift) with nearly identical shifting extent to
8 those observed using Ag NPs, confirming the robustness of ^{15}N -induced SERS shift and
9 independence of NPs type. Ag NPs exhibited superior SERS enhancement over Au NPs,
10 as observed from the much better signal-to-noise ratio, however, Ag NPs are toxic to a
11 great variety of bacteria and can affect SERS features of bacteria.^{20,30,33} In order to
12 examine the possible effect of Ag toxicity on ^{15}N -induced Raman shifts, SERS spectra of
13 bacteria were obtained by adding different concentrations of Ag NPs (Figure 3). The
14 relative intensity in all three ^{15}N percentages changed remarkably with the concentration
15 of Ag NPs increasing, due to the biochemical responses of bacteria to Ag NPs.²⁰ However,
16 SERS bands position remained unchanged, such as the constant 717 cm^{-1} (^{15}N 98.0%),
17 720 (^{15}N 73.6%), and 730 cm^{-1} (^{15}N 0.4%) bands in different Ag concentrations (Figure
18 3), but solely depended on the ^{15}N isotopic enrichments in bacteria. This demonstrated
19 that Ag NPs were suitable for investigating ^{15}N stable isotope probing regardless of its
20 toxicity.

21 The high-quality SERS spectra allowed us to establish a linear relationship ($R^2 = 0.93 -$
22 0.99) between shift extent and ^{15}N - NH_4Cl percentage in a total of six SERS bands
23 (Figure 4), in contrast to the only one linear ^{15}N -induced shifting band in previous

work.¹¹ The sharp bands with a pronounced shift such as 653, 730, 957 cm^{-1} showed a high degree of correlation ($R^2 = 0.98$ or 0.99), demonstrating their potential to sensitively indicate nitrogen assimilation into bacterial biomass. This is a great advantage of SERS over normal Raman spectra which still lack a clear biomarker band of ^{15}N assimilation. The linear shifting also allows sensitive estimation of the extent of nitrogen assimilation and ^{15}N -isotope incorporation strength by bacteria.

^{15}N -induced shifts were also observed in typical environmental bacterium of gram-negative *P. putida* KT2440 and gram-positive *B. megaterium* (Figure S1). Premasiri et al also reported very similar shift in gram-positive *S. aureus* and *B. anthracis* grown in ^{15}N and ^{14}N media.²⁶ These works demonstrated that SERS combined with ^{15}N -labeling was universally applicable to probe nitrogen assimilation in different bacteria. Particularly, the band at 730 cm^{-1} was distinguishably sharp with a consistent position and as large as 13 cm^{-1} shift (Figure 2 and 4), and thus can be used as a universal Raman biomarker to identify ^{15}N -labeled cells and compare bacterial activity, even in a complex microbial community containing diverse bacterial species.

The above facts demonstrate that SERS- ^{15}N SIP is a highly robust, sensitive and non-destructive technique capable of unambiguously indicating nitrogen assimilation across diverse bacteria.

Interpretation of SERS bands related to ^{15}N stable isotope probing

Table 1 summarizes all the shifted and non-shifted SERS bands induced by ^{15}N assimilation. All shifted bands were found to be from nitrogen-associated compounds. Among them, 730 and 1325 cm^{-1} bands were assigned to adenine-containing biomolecules, which have been well demonstrated by Premasiri et al and also supported

1 by other bacterial SERS works.^{20,26,27} Adenine contains four nitrogen atoms in its ring
2 structure and one nitrogen atom in side chain. This explains the significant shift in 730
3 cm^{-1} band when ‘heavier’ ^{15}N substitutes the ‘lighter’ ^{14}N in adenine. By comparison,
4 bands from guanine-related ($\sim 660 \text{ cm}^{-1}$) and cytosine-related (793 cm^{-1}) biomolecules
5 displayed a small shift of 9 and 5 cm^{-1} , respectively (Figure 2 and Table 1). Guanine and
6 cytosine contain four and three nitrogen atoms in their ring structure respectively,
7 contributing to the observed ^{15}N -corresponding shift. The observed larger shift in adenine
8 than guanine and cytosine could be due to the more abundant and active biomolecules
9 possessing adenine-moiety in cells, such as ATP and NADP, NADPH. Therefore, ^{15}N may
10 have more chance to be incorporated into adenine-containing molecules.

11 A majority of cellular nitrogen can be also found in protein containing amide group.
12 Previous work demonstrated the presence of ^{15}N in protein during bacterial growth.⁵
13 However, protein-associated shifts were only observed in SERS bands of 1216 or 1206
14 cm^{-1} (Amide III of protein), but not obvious in 1002 (Phenylalanine), 1624 and 1682 cm^{-1}
15 (Amide I of protein). The 1002 cm^{-1} band was assigned to benzene ring-breathing
16 vibration of phenylalanine.³⁴ The only one nitrogen of phenylalanine is in the side alkyl
17 chain of benzene ring, and thus may exert little effect on ring-breathing vibration,
18 explaining its non-shift feature. SERS bands of 1624 and 1682 cm^{-1} were assigned to
19 amide vibration associated with α -helix and β -sheet which are the secondary protein
20 structure,³⁵ and thus could be not sensitive enough to ^{15}N substitution. Notably, 1031
21 ($=\text{C-H}$ bending), 1459 (CH_2 deformation), and 1580 cm^{-1} ($\text{C}=\text{C}$ stretching) bands that did
22 not involve nitrogen displayed no shift with ^{15}N substitution in biomass.³⁵ Although
23 protein-related bands were not sensitive enough following ^{15}N assimilation, the

1 prominent shifts in adenine- and other nucleotides-related biomolecules still hold
2 potentials to enhance our understanding of some important nitrogen-related biochemical
3 processes, such as ATP synthesis and nucleic acid metabolism.

4 **The applicability of SERS-¹⁵N SIP in N₂-fixing bacteria and environmental** 5 **microorganisms**

6 The applicability of SERS-¹⁵N SIP was also examined in important N₂-fixing bacteria
7 (via ¹⁵N₂ incubation), which are capable of converting inert atmospheric nitrogen to
8 bioavailable ammonia or other molecules to living organisms and thus play an important
9 role in nitrogen cycle. Normal Raman spectra of *A. chroococcum* show clear Raman
10 bands of cytochrome c (Figure. S2), which is used for nitrogen fixation of *A.*
11 *chroococcum*. SERS spectra of N₂-fixing bacteria of *A. chroococcum* incubated with ¹⁵N₂
12 displayed a prominent 13 cm⁻¹ shift from that with air (¹⁴N₂) controls due to ¹⁵N
13 assimilation, such as the Raman shifts from 730 to 717 cm⁻¹ and from 1325 to 1312 cm⁻¹
14 (Figure 5A), the same as the results with ¹⁵NH₄Cl incubation (Figure 2). This indicates
15 that SERS-¹⁵N SIP should be applicable to any nitrogen assimilation including N₂.

16 Furthermore, we also applied SERS-¹⁵N SIP to probe environmental microbial
17 community by amending three different nitrogen sources of ¹⁵NH₄Cl, ¹⁵NO₃, and ¹⁵N₂
18 into water sampled from Xinglin Bay (Figure 5B) which is an important wetland resource
19 in Xiamen city. In this environmental sample, two strong carotenoid bands at 1155 and
20 1514 cm⁻¹ were observed in both SERS (a-f) and normal Raman spectra (g, h) due to the
21 resonance Raman effect of carotenoid, which has been frequently detected in
22 environmental microorganisms, especially of photosynthetic bacteria.³⁶ In addition,
23 double bands at 730 and 716 cm⁻¹ were clearly observed for ¹⁵NH₄Cl incubation (Figure

5B). The 730 cm^{-1} band was the same as that incubated with $^{14}\text{NH}_4\text{Cl}$, and the 716 cm^{-1} band was identical to the pure culture incubated with $^{15}\text{NH}_4\text{Cl}$ (Figure 2), suggesting that environmental microorganisms assimilated $^{15}\text{NH}_4\text{Cl}$. The simultaneous presence of 730 and 716 cm^{-1} bands demonstrated different activities of environmental bacteria in assimilating $^{15}\text{NH}_4\text{Cl}$ and ^{14}N nitrogen source existing in the natural water body. This clearly indicated the diversity of microorganisms in Xinglin Bay, and also pointed to the necessity to identify active environmental cell at a high resolution single-cell level. By comparison, no obvious shifts were observed for $^{15}\text{NO}_3$ and $^{15}\text{N}_2$ incubation. For $^{15}\text{NO}_3$, the reason could be related to the lack of denitrifying bacteria in the surface water sampled from Xinglin Bay, as the surface water is in good contact with air and thus adverse for the growth of denitrifying bacteria. For $^{15}\text{N}_2$, the reason could be related to the presence of other more easily bioavailable nitrogen sources in Xinglin Bay water considering the sewage disposal from surrounding dwelling and business area.

Single-cell SERS study of nitrogen assimilation

A study at single-cell level can reveal specific properties of heterogeneity and spatial relationship of individual cells that bulk measurement cannot achieve, and also provides a way to circumvent cultivation and study those yet nonculturable bacteria in natural environment.⁸ Here, in order to extend SERS- ^{15}N SIP from bulk to single-cell level, we developed a simple and effective method to prepare sample by mixing an optimized ratio of Ag NPs with cell suspension. From the microscopic view (Figure 6), single cell in partial contact with aggregated Ag NPs was clearly observed. Interestingly, SERS signal can only be obtained when focusing laser on the position of Ag NPs in contact with cell (top blue spectrum in Figure 6), but became very weak on the same cell without clear

1 contact with Ag NPs (bottom red spectrum in Figure 6), under the same acquisition
2 condition. This observation is in good agreement with the short-distance enhancement
3 effect of SERS which only allows substances adsorbed or in close proximity to
4 nanostructures to be enhanced.³⁷ The obtained SERS from the single cell displayed a
5 strong and sharp band at 730 cm^{-1} , the same as that observed in bulk SERS spectra of
6 bacteria, demonstrating that single-cell SERS spectra were able to detect
7 nitrogen-associated band.

8 Single-cell SERS spectra were also acquired from *E. coli* fed with $^{15}\text{NH}_4\text{Cl}$ of different
9 percentages (Figure 7A). The sharp band at 730 cm^{-1} shifted linearly with the increasing
10 ^{15}N percentages in cell growth media (Figure 7B). The linear relationship in both bulk
11 and single-cell measurement was very close; both had a linear slope of around 0.14 and
12 shift extent of 13 cm^{-1} (Figure 4 and 7), demonstrating that SERS was able to study
13 nitrogen assimilation at single-cell level. The detection limit of SERS was 24.8% for ^{15}N
14 incorporation ($p < 0.05$), at which significant band shift can be clearly observed. Given
15 that the chance of ^{15}N incorporation into single cells is random, ^{15}N content in single cells
16 should be proportional to ^{15}N percentage in medium.

17 The developed single-cell preparation method not only allowed SERS- ^{15}N SIP to be
18 performed at explicitly single-cell level, but also benefited single cell isolation via the
19 recently developed Raman activated cell ejection due to the partial contact of single cell
20 with nanoparticles.¹⁴ This technique can isolate single cell of interest, in this case cells
21 related to nitrogen assimilation, from Al-coated slide and allow down-stream process of
22 single-cell genomics.

23 CONCLUSIONS

We demonstrated that SERS combined with ^{15}N -stable isotope labelling can be used as a non-destructive, reproducible, and universally applicable approach to monitor nitrogen assimilation in different types of bacteria at both bulk and single-cell level, and from pure culture to environmental microbial community. ^{15}N -assimilation in cells induced a much clearer Raman shifts in SERS than normal Raman. The shifts were highly reproducible and robust, and presented a linear relationship with the ^{15}N -content in both bulk and single cell, irrespective of nanoparticle type (Ag or Au) and concentrations. The shift extent varied in different SERS bands. Among them, 730 cm^{-1} band was found to be the best indicator of nitrogen assimilation due to its reproducibility, prominent shift, strong intensity, and sharp band shape. The developed SERS- ^{15}N SIP approach was also applied in important N_2 -fixing bacteria via $^{15}\text{N}_2$ incubations, and the same prominent band shift as that induced by $^{15}\text{NH}_4\text{Cl}$ was observed, demonstrating the applicability of SERS- ^{15}N SIP to different nitrogen sources. SERS- ^{15}N SIP was further applied to environmental microbial community from a local wetland water source via three types of nitrogen incubation, including $^{15}\text{NH}_4\text{Cl}$, $^{15}\text{NO}_3$, and $^{15}\text{N}_2$. Bacteria in the natural water were demonstrated to assimilate $^{15}\text{NH}_4\text{Cl}$, but not $^{15}\text{NO}_3$ and $^{15}\text{N}_2$, possibly due to the lack of denitrifying bacteria in the surface water of wetland and the presence of bioavailable nitrogen source. In addition, different activities of environmental bacteria in assimilating $^{15}\text{NH}_4\text{Cl}$ were demonstrated. This nitrogen source-dependent and bacteria-dependent activity in nitrogen assimilation indicated the diversity of microbial community and pointed to the necessity of single-cell level characterization. By developing a simple method of mixing an optimized ratio of bacteria with nanoparticles, SERS- ^{15}N SIP was further extended to an explicit high-resolution single-cell level.

1 The future development and application SERS-¹⁵N SIP can be high-throughput
 2 identification of functional bacteria such as N₂-fixing and N-containing
 3 pollutants-degrading bacteria in a complex microbial community at single-cell level. The
 4 non-destructive detection also allows isolation of single cell and the following genomic
 5 analysis, which will facilitate linking of bacterial phenotype with genotype and thus
 6 provide more insights into the role of microbes in the biogeochemical cycling of nitrogen.

7 References

- 8 (1) Hoffman, B. M.; Lukoyanov, D.; Yang, Z. Y.; Dean, D. R.; Seefeldt, L. C. *Chem Rev* **2014**, *114*, 4041-4062.
- 9 (2) Woebken, D.; Burow, L. C.; Behnam, F.; Mayali, X.; Schintlmeister, A.; Fleming, E. D.; Prufert-Bebout, L.;
 10 Singer, S. W.; Corte's, A. L. p.; Hoehler, T. M.; Pett-Ridge, J.; Spormann, A. M.; Wagner, M.; Weber, P. K.;
 11 Bebout, B. M. *ISME J.* **2014**, 1-12.
- 12 (3) Eichorst, S. A.; Strasser, F.; Woyke, T.; Schintlmeister, A.; Wagner, M.; Woebken, D. *FEMS Microbiol. Ecol.*
 13 **2015**, *91*, fiv106.
- 14 (4) McGlynn, S. E.; Chadwick, G. L.; Kempes, C. P.; Orphan, V. J. *Nature* **2015**, *526*, 531-535.
- 15 (5) Kruger, M.; Wolters, H.; Gehre, M.; Joye, S. B.; Richnow, H. H. *FEMS Microbiol. Ecol.* **2008**, *63*, 401-411.
- 16 (6) Zhou, G. W.; Yang, X. R.; Li, H.; Marshall, C. W.; Zheng, B. X.; Yan, Y.; Su, J. Q.; Zhu, Y. G. *Environ. Sci.*
 17 *Technol.* **2016**, *50*, 9298-9307.
- 18 (7) Amann, R. I.; Ludwig, W.; Schleifer, K. H. *Microbiol Rev* **1995**, *59*, 143-169.
- 19 (8) Huang, W. E.; Song, Y.; Xu, J. *Microb Biotechnol* **2015**, *8*, 15-16.
- 20 (9) Berry, D.; Mader, E.; Lee, T. K.; Woebken, D.; Wang, Y.; Zhu, D.; Palatinszky, M.; Schintmeister, A.;
 21 Schmid, M. C.; Hanson, B. T.; Shterzer, N.; Mizrahi, I.; Rauch, I.; Decker, T.; Bocklitz, T.; Popp, J.; Gibson, C.
 22 M.; Fowler, P. W.; Huang, W. E.; Wagner, M. *Proc. Natl. Acad. Sci. U. S. A.* **2015**, *112*, E194-E203.
- 23 (10) Huang, W. E.; Stoecker, K.; Griffiths, R.; Newbold, L.; Daims, H.; Whiteley, A. S.; Wagner, M. *Environ.*
 24 *Microbiol.* **2007**, *9*, 1878-1889.
- 25 (11) Wang, Y.; Huang, W. E.; Cui, L.; Wagner, M. *Curr. Opin. Biotechnol.* **2016**, *41*, 34-42.
- 26 (12) Maquelin, K.; Kirschner, C.; Choo-Smith, L. P.; van den Braak, N.; Endtz, H. P.; Naumann, D.; Puppels, G.
 27 *J. J. Microbiol. Methods* **2002**, *51*, 255-271.
- 28 (13) Huang, W. E.; Griffiths, R. I.; Thompson, I. P.; Bailey, M. J.; Whiteley, A. S. *Anal. Chem.* **2004**, *76*,
 29 4452-4458.
- 30 (14) Song, Y. Z.; Kaster, A. K.; Vollmers, J.; Song, Y. Q.; Davison, P. A.; Frentrup, M.; Preston, G. M.;
 31 Thompson, I. P.; Murrell, J. C.; Yin, H. B.; Hunter, C. N.; Huang, W. E. *Microb Biotechnol* **2017**, *10*, 125-137.
- 32 (15) Muhamadali, H.; Chisanga, M.; Subaihi, A.; Goodacre, R. *Anal. Chem.* **2015**, *87*, 4578-4586.
- 33 (16) Stiles, P. L.; Dieringer, J. A.; Shah, N. C.; Van Duyne, R. R. *Annu Rev Anal Chem* **2008**, *1*, 601-626.
- 34 (17) Kneipp, J.; Kneipp, H.; Kneipp, K. *Chem. Soc. Rev.* **2008**, *37*, 1052-1060.
- 35 (18) Kubryk, P.; Kolschbach, J. S.; Marozava, S.; Lueders, T.; Meckenstock, R. U.; Niessner, R.; Ivleva, N. P.
 36 *Anal. Chem.* **2015**, *87*, 6622-6630.
- 37 (19) Walter, A.; Marz, A.; Schumacher, W.; Rosch, P.; Popp, J. *Lab Chip* **2013**, *11*, 1013-1021.
- 38 (20) Cui, L.; Chen, P.; Chen, S.; Yuan, Z.; Yu, C.; Ren, B.; Zhang, K. *Anal. Chem.* **2013**, *85*, 5436-5443.
- 39 (21) Cui, L.; Chen, P. Y.; Zhang, B. F.; Zhang, D. Y.; Li, J. Y.; Martin, F. L.; Zhang, K. S. *Water Res.* **2015**, *87*,
 40 282-291.
- 41 (22) Chen, P. Y.; Cui, L.; Zhang, K. S. *J. Membr. Sci.* **2015**, *473*, 36-44.
- 42 (23) Jarvis, R. M.; Goodacre, R. *Chem. Soc. Rev.* **2008**, *37*, 931-936.
- 43 (24) Premasiri, W. R.; Moir, D. T.; Klempner, M. S.; Krieger, N.; Jones, G.; Ziegler, L. D. *J. Phys. Chem. B* **2005**,

109, 312-320.
(25) Cui, L.; Zhang, Y.-J.; Huang, W. E.; Zhang, B.-F. M., Francis L; Li, J.-Y.; Zhang, K.-S.; Zhu, Y.-G. *Anal. Chem.* **2016**, *88*, 3164–3170.
(26) Premasiri, W. R.; Lee, J. C.; Sauer-Budge, A.; Th  berge, R.; Costello, C. E.; Ziegler, L. D. *Anal. Bioanal. Chem.* **2016**, *408*, 4631-4647.
(27) Kubryk, P.; Niessner, R.; Ivleva, N. P. *Analyst* **2016**, *141*, 2874-2878.
(28) Zhang, D. Y.; Berry, J. P.; Zhu, D.; Wang, Y.; Chen, Y.; Jiang, B.; Huang, S.; Langford, H.; Li, G. H.; Davison, P. A.; Xu, J.; Aries, E.; Huang, W. E. *ISME J.* **2015**, *9*, 603-614.
(29) Cui, L.; Yao, M.; Ren, B.; Zhang, K.-S. *Anal. Chem.* **2011**, *83*, 1709-1716.
(30) Cui, L.; Chen, S. D.; Zhang, K. S. *Spectrochim. Acta A* **2015**, *137*, 1061-1066.
(31) Wang, Y.; Ji, Y. T.; Wharfe, E. S.; Meadows, R. S.; March, P.; Goodacre, R.; Xu, J.; Huang, W. E. *Anal. Chem.* **2013**, *85*, 10697-10701.
(32) Han, X. X.; Huang, G. G.; Zhao, B.; Ozaki, Y. *Anal. Chem.* **2009**, *81*, 3329-3333.
(33) El-Zahry, M. R.; Mahmoud, A.; Refaat, I. H.; Mohamed, H. A.; Bohlmann, H.; Lendl, B. *Talanta* **2015**, *138*, 183-189.
(34) Li, M. Q.; Huang, W. E.; Gibson, C. M.; Fowler, P. W.; Jousset, A. *Anal. Chem.* **2013**, *85*, 1642-1649.
(35) Talari, A. C. S.; Movasaghi, Z.; Rehman, S.; Rehman, I. U. *Appl. Spectrosc. Rev.* **2014**, *50*, 46-111.
(36) Li, M. Q.; Canniffe, D. P.; Jackson, P. J.; Davison, P. A.; FitzGerald, S.; Dickman, M. J.; Burgess, J. G.; Hunter, C. N.; Huang, W. E. *ISME J.* **2012**, *6*, 875-885.
(37) Tian, J. H.; Liu, B.; Li, X. L.; Yang, Z. L.; Ren, B.; Wu, S. T.; Tao, N. J.; Tian, Z. Q. *J. Am. Chem. Soc.* **2006**, *128*, 14748-14749.
(38) Ivleva, N. P.; Wagner, M.; Szkola, A.; Horn, H.; Niessner, R.; Haisch, C. *J. Phys. Chem. B* **2010**, *114*, 10184-10194.

Supporting information

Additional information as noted in text. This material is available free of charge via the Internet at <http://pubs.acs.org>.

Author information

Corresponding Author

*E-mail, lcui@iue.ac.cn. Phone: 86-5926190560.

*E-mail, wei.huang@eng.ox.ac.uk. Phone: 44-1865283786.

The authors declare no competing financial interest.

Acknowledgments

This work was supported by the Strategic Priority Research Program of Chinese Academy of Sciences (XDB15020302, XDB15020402), China Scholarship Council, and Youth Innovation Promotion Association of Chinese Academy of Sciences. WEH acknowledge support from EPSRC (EP/M02833X/1), NERC (NE/M002934/1).

1 **Figure Legends**

2 **Figure 1.** Normal Raman spectra of unlabelled and fully labelled single *E. coli* cell with
3 different stable isotopes of ^2D , ^{13}C , and ^{15}N .

4 **Figure 2.** SERS spectra of *E. coli* grown in media amended with different percentages of
5 $^{15}\text{N-NH}_4\text{Cl}$ using Ag NPs (A) and Au NPs (B) to enhance Raman signal.

6 **Figure 3.** SERS spectra of *E. coli* grown in media containing 98.0% (A), 73.6% (B), and
7 0.4% (C) of $^{15}\text{N-NH}_4\text{Cl}$ using different concentrations of Ag NPs to enhance Raman
8 signal.

9 **Figure 4.** SERS band shifts of *E. coli* with respect to the $^{15}\text{N-NH}_4\text{Cl}$ percentage in culture
10 media. A linear regression between band shift and $^{15}\text{N-NH}_4\text{Cl}$ percentage is shown in red.
11 R^2 and shift extent (δ) are indicated for each band.

12 **Figure 5.** (A) SERS spectra of N_2 -fixing *A. chroococcum* incubated with $^{15}\text{N}_2$ and $^{14}\text{N}_2$.
13 (B) SERS spectra of environmental microbial community from a local wetland water
14 incubated with different nitrogen sources indicated. The bottom two curves (g, h) are
15 normal Raman spectra of single bacteria from the same wetland water.

16 **Figure 6.** Single-cell SERS spectra from a single *E. coli* cell with (blue spectrum) and
17 without (red spectrum) contact with Ag NPs as illustrated in the microscopic view. The
18 green dot indicates the position where laser spot focused on the sample.

19 **Figure 7.** (A) Single-cell SERS spectra of *E. coli* grown in media amended with different
20 percentages of $^{15}\text{N-NH}_4\text{Cl}$. (B) Shift of SERS band at 730 cm^{-1} with respect to the ^{15}N
21 percentage. A linear regression between band shift and $^{15}\text{N-NH}_4\text{Cl}$ percentage is shown in
22 red ($R^2 = 0.96$, δ (shift extent) = 13 cm^{-1}).

23

1 **Table 1.** ^{15}N -induced shift in SERS bands of bacteria and tentative band
2 assignments.^{20,27,35,38}

<i>E. coli</i>		<i>P. putida</i>		<i>B. megaterium</i>		Tentative band assignments
Band cm^{-1}	Shift cm^{-1}	Band cm^{-1}	Shift cm^{-1}	Band cm^{-1}	Shift cm^{-1}	
653	9			662	9	Ring breathing of guanine-containing compounds
730	13	730	13	730	13	ring breathing of adenine-containing compounds
793	5	793	5	793	5	ring breathing of cytosine-containing compounds
957	19			957	15	C-N stretching
		1133	20			C-N stretching
1216	6	1206	11			Amide III of protein
1325	13	1325	13	1325	13	adenine-containing compounds
1000	0	1000	0			Ring breathing of phenylalanine
1031	0	1031	0	1031	0	=C-H bending
1459	0	1459	0	1457	0	CH_2 deformation
1581	0	1585	0	1579	0	C=C stretching
1632	0	1649	0	1632	0	Amide I (α -helix)
				1682	0	Amide I (β -sheet)

3
4
5

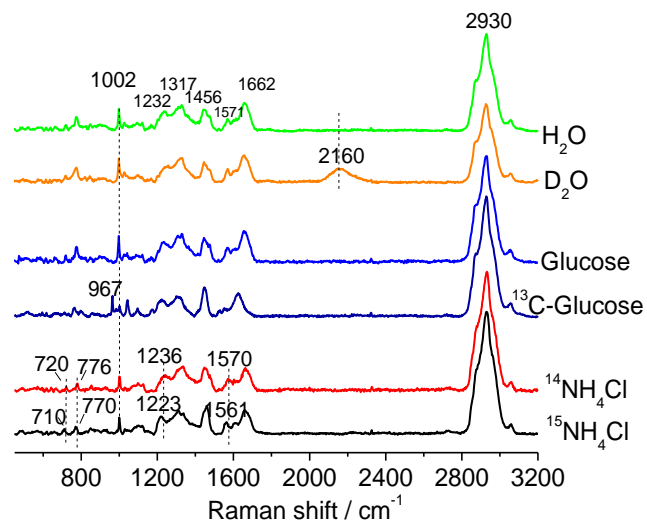


Figure 1

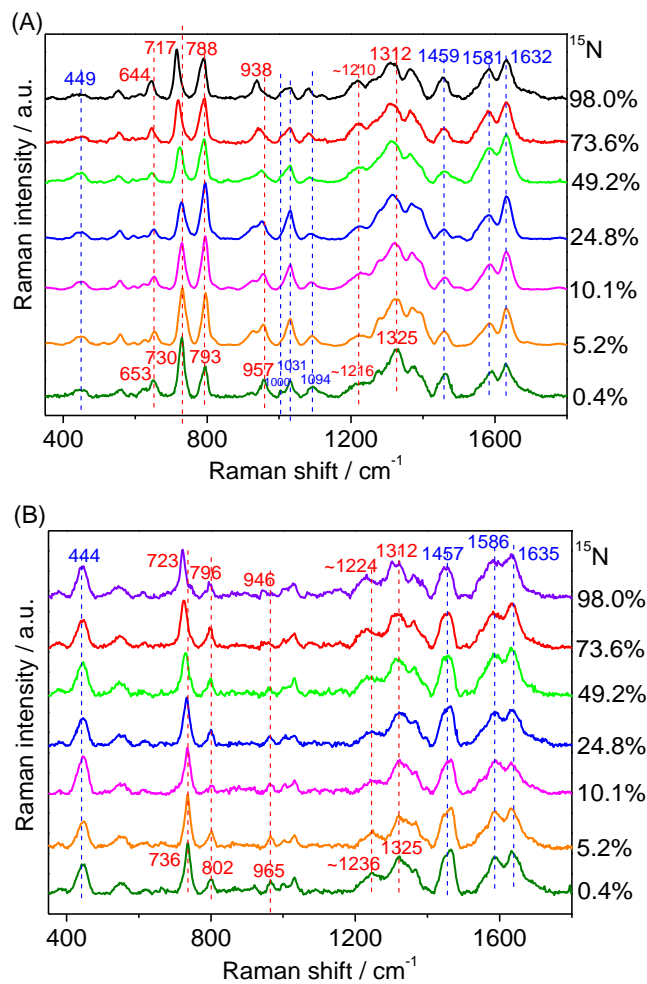


Figure 2

1

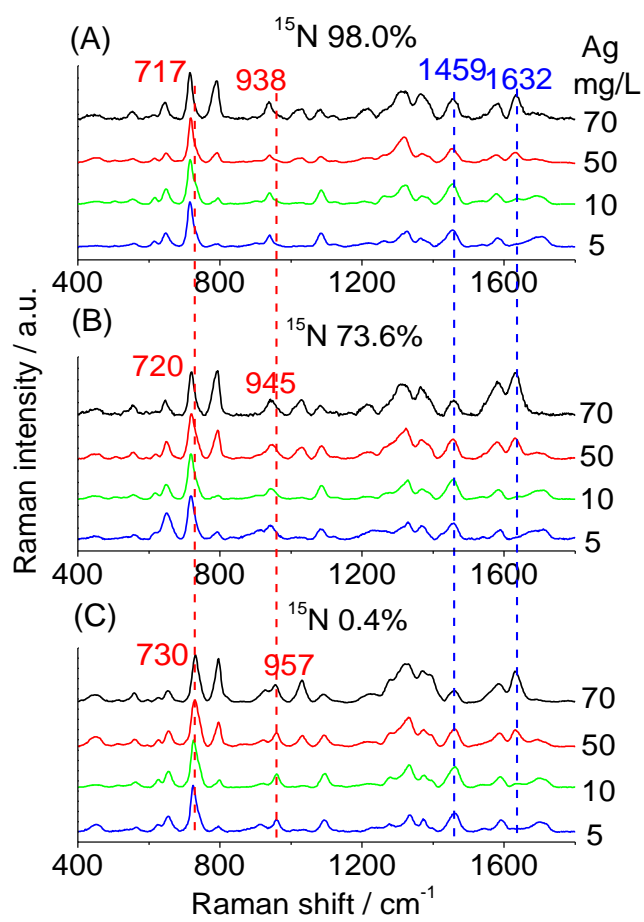
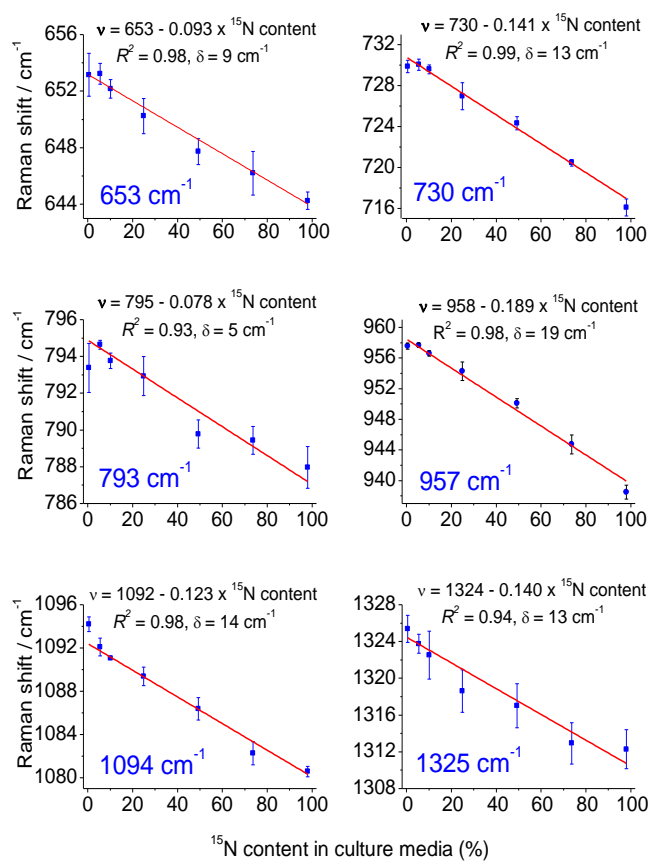


Figure 3

1

2



3

4

Figure 4

5

6

7

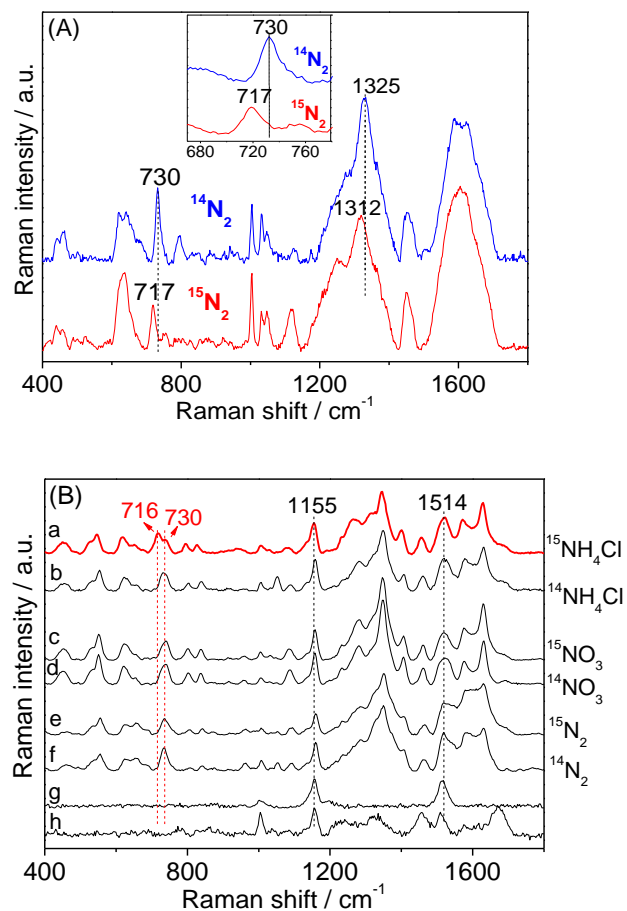
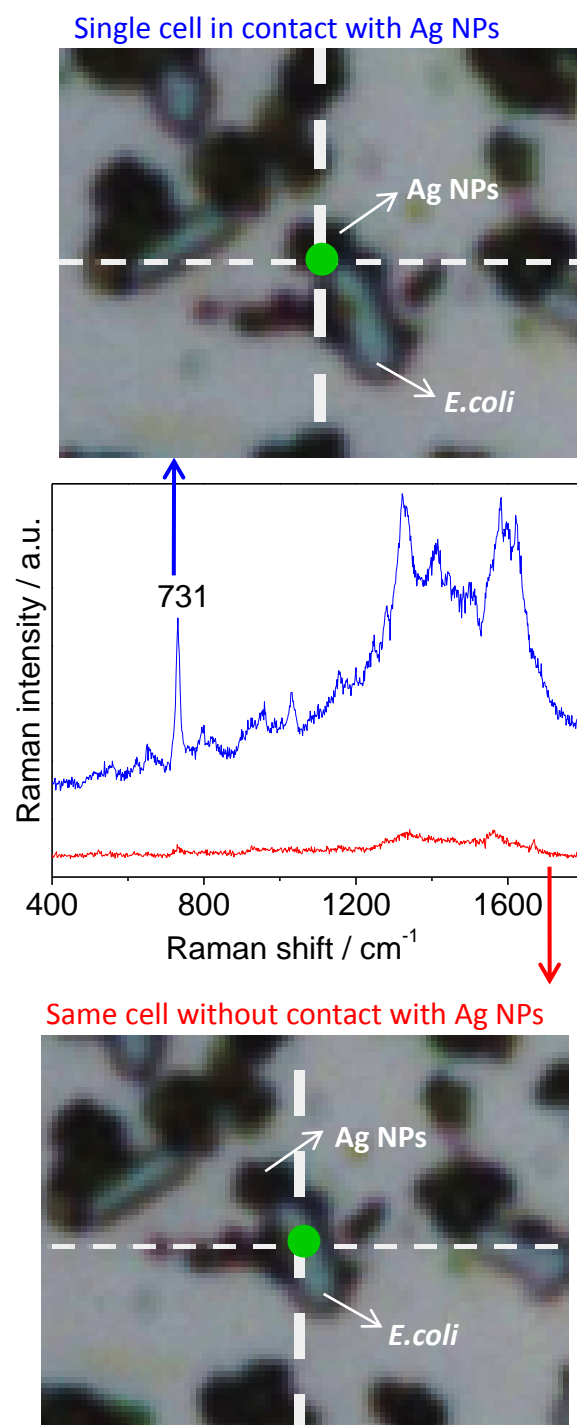


Figure 5

1

2



3

4

5

Figure 6

1

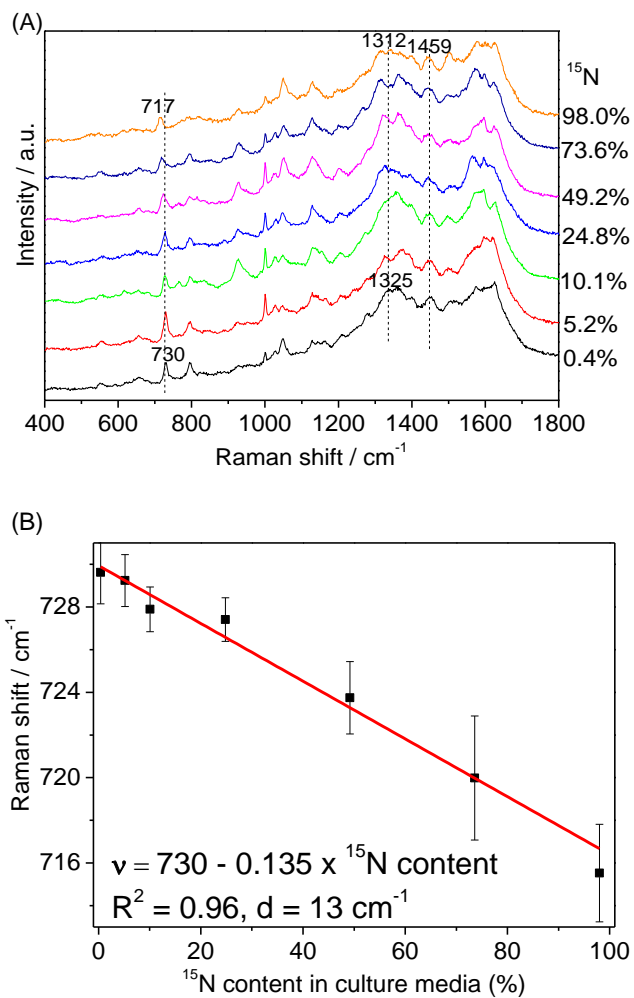


Figure 7